Supporting information for

Phototriggered Base Proliferation: A Highly Efficient Domino Reaction for Creating Functionally Photo-Screened Materials†

Minghui He,[a,b] Xun Huang,[a] Zhaohua Zeng [a] and Jianwen Yang*[a]

[a]Institute of Polymer Science, DSAPM Lab, School of Chemistry and Chemical Engineering, Sun Yat-Sen University, Guangzhou, 510275, China. E-mail: cesyjw@mail.sysu.edu.cn; Fax: +86-20-84111138; Tel: +86-20-84111138;

[b]State Key Laboratory of Pulp & Paper Engineering, South China University of Technology, Guangzhou, 510640, China

Content

1 UV spectrum of QA-DBU

Absorption characteristic of QA-DBU was investigated by UV-Vis spectroscopy (Figure s1). As can be seen, QA-DBU exhibits good absorption characteristics with two peaks at 196 nm and 224 nm and a tail over 300 nm.

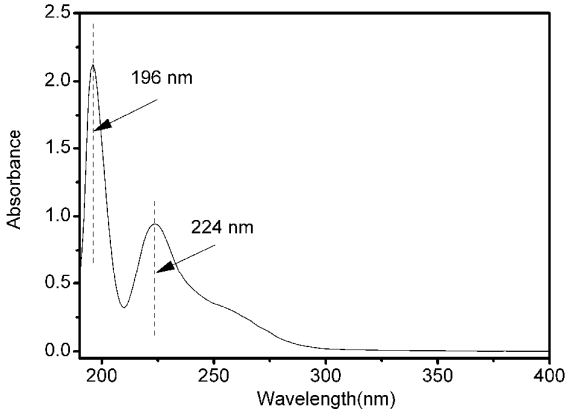

Figure s1 UV-vis absorption spectra of QA-DBU in AN (1×10^{-5} M).

2 Physically diffuse amines-controlled self-propagating polymerization.

First, we investigated the self-propagating polymerization based on the photocaged superbase and readily available peroxides (Figure s2, Figure s3). For the given dimensions (60×3 mm), the irradiation time to initiate self-propagating polymerization (the induction period, T_{start}) was 0.35 min and the non-irradiated region was polymerized within 0.9 min. Figure 3 shows a nonlinear dependence of spreading velocity (V) on time. Namely, V first undergoes a gradual increase, and then begins to sharply decrease around 0.75 min. In order to explore the mechanism of nonlinear propagation, we detected the physical diffusion of photogenerated DBU by ESI-MS. Interestingly, the protonated DBU^+ (m/z =153.3) at 2.5 cm radius region was detected because of the self-enrichment of superbases from irradiated areas toward the non-irradiated areas during polymerization, as shown in Figure s4. Therefore, it could be envisioned that the concentration of the diffuse superbases at the polymerization front will gradually reduce because of the corresponding increase of frontal area during polymerization, thus decreases the spreading velocity.

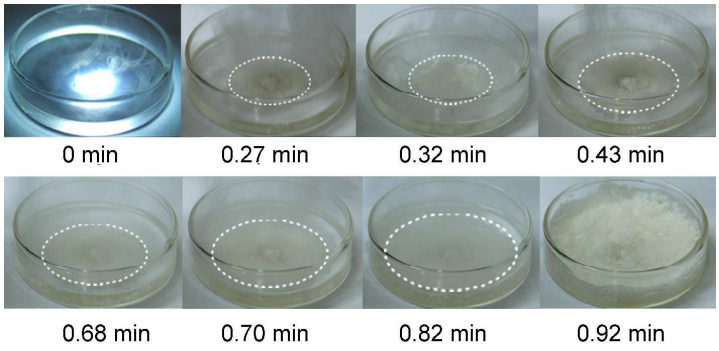

Figure s2 Sequence of image-processed video-frames illustrating the self-propagating polymerization. Experimental conditions: [QA-DBU] = 1.1×10^{-4} mol, [BPO] = 5.5×10^{-4} mol, DMSO = 2.5 mL, TMPTA = 4 g, AA=1g.

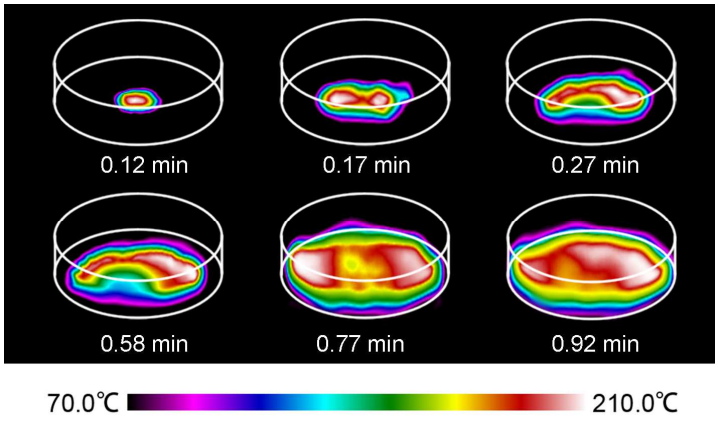

Figure s3 A representative time series of the IR thermal montages illustrating the self-propagating polymerization measured by an infrared (IR) thermal imaging camera.

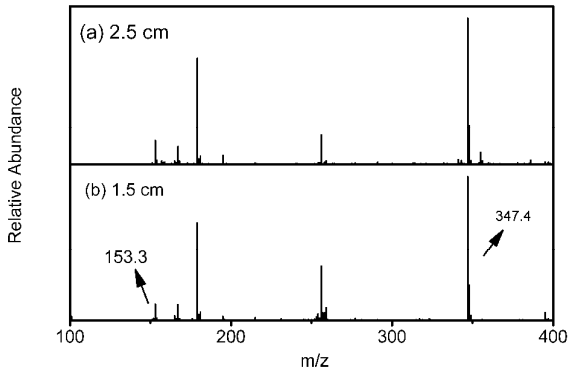

Figure s4 Positive ion ESI-MS spectra of the polymer in DMSO at different radii: (a) 2.5 cm, (b) 1.5 cm. Experimental conditions: [QA-DBU] = 1.1×10^{-4} mol, [BPO] = 5.5×10^{-4} mol, DMSO = 2.5 mL, TMPTA = 4 g, AA=1g.

In order to obtain the spatial temperature profiles, we measured temperature by an infrared (IR) thermal imaging camera, allocating three positions along the radial direction of the reactor; *e.g.* T1, T2 and T3 at *ca.* 0.5, 1.5 and 2.5 cm, respectively. Because of the decreased superbase concentration along the radial direction, the maximum temperature of the front (T_{max}) at three different positions increases from 137 °C, 160 °C to 165 °C, as indicated in Figure s5. It is worth noting that instable front temperature is not usable to synthesize advanced materials.

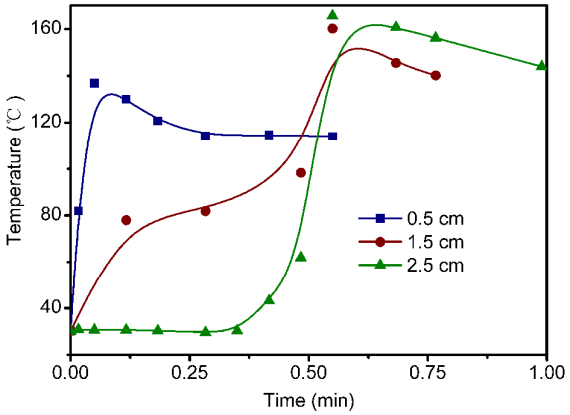

Figure s5. Plot of temperature profiles at different radii vs time of propagation recorded during the self-propagating polymerization based on physically diffuse amines. Experimental conditions: [QA-DBU] = 1.1×10^{-4} mol, [BPO] = 5.5×10^{-4} mol, DMSO = 2.5 mL, TMPTA = 4 g, AA=1g.

The synergistic efficiency of physical diffusion system to sustain a traveling front was evaluated. Figure s6 shows spreading velocity *vs* time for different [BPO]:[QA-DBU] ratios. For lower BPO concentration (3:1), no propagation occurred (Figure s6e), but an increase of BPO concentration from 5:1 to 7.5:1 causes a remarkable increase of spreading velocity (Figure s6d and s6c). The higher velocities result from much more photogenerated DBU which accelerates the decomposition of BPO. However, for higher values (10:1, Figure s6b), spreading velocity begins to decrease, and even could not be sustained for 15:1 (Figure s6a). Maybe this is because high BPO concentration greatly accelerates the initial photopolymerization, but restrains the physical diffusion of amine, thus no propagation occurred. Consequently, although front temperature was over 137 °C, BPO alone thermal-initiation cannot sustain the self-propagating polymerization. Because photogenerated superbases can be driven from irradiated areas toward the non-irradiated areas during polymerization, the amine-diffusion controlled redox initiation should facilitate the propagation polymerization.

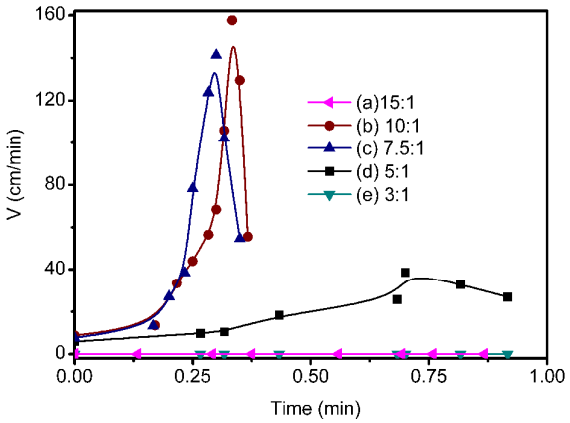

Figure s6 Spreading velocity vs time for different [BPO]:[QA-DBU] ratios: (a) 15:1, (b) 10:1, (c) 7.5:1, (d) 5:1, (e) 3:1, [QA-DBU] = 1.1×10^{-4} mol, DMSO = 2.5 mL, TMPTA = 4 g, AA=1g.

Table s1 The local maximum temperature ($T_{l\text{-}max}$) *vs* [BPO]:[QA-DBU] ratio

[BPO]:[QA-DBU] ratio	$T_{l\text{-}max}$ (°C)	Observation
3:1	-	No propagation
5:1	240.2	Fast propagation
7.5:1	242.1	Fast propagation
10:1	187.1	Fast propagation
15:1	-	No propagation

Experimental conditions: [QA-DBU] = 1.1×10^{-4} mol, DMSO = 2.5 mL, TMPTA = 4 g, AA=1g.

As mentioned above, due to the inhomogeneous diffusion of the superbase from the center to the propagating front, local high temperature areas appeared during polymerization, which are harmful for preparing thermal sensitive materials. It thus could be predicted that the obtained polymer material would exhibit poor homogeneity and mechanical performance. The local maximum temperature ($T_{l\text{-}max}$) is listed in Table s1 as a function of [BPO]:[QA-DBU] ratio, within the above range of BPO concentration causing self-propagating polymerization to occur. It should be emphasized that the $T_{l\text{-}max}$ is about 240 °C for 5:1 or 7.5:1, and 187 °C for 10:1.

3 Base proliferation in solution.

Figure s7 shows a series of ^{1}H NMR spectral changes of BA-BPD in DMSO-d_6 (100 mmol L^{-1}) in the absence of and presence of 4-benzylpiperidine (5 mmol L^{-1}) at 25 °C. Amine-catalyzed decomposition of BA-BPD was followed by monitoring the disappearing proton signals of methylene (H_a, 4.23 ppm) and appeared proton signals of vinyl group (H_b, 6.25 ppm). Before addition of amine (Figure s7a), the proton H_b,

assigning to the vinyl groups, was not observed until the presence of 4-benzylpiperidine (Figure s7b). After prolonged reaction, the proton signals gradually appeared (Figure s7c).

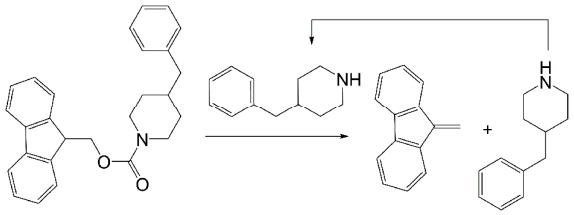

Scheme s1 Autocatalytic decomposition of BA-BPD.

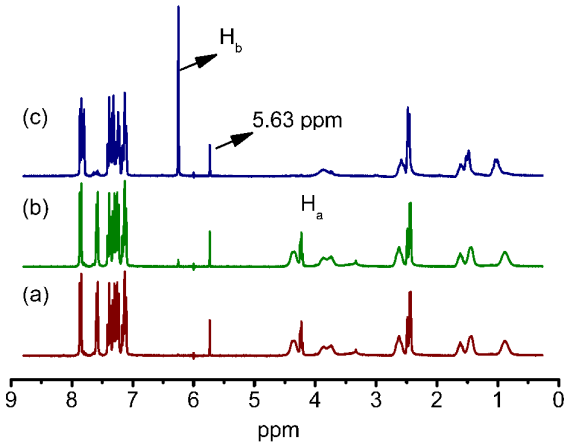

Figure s7 ^{1}H NMR spectral changes of BA-BPD in DMSO-d_6 (100 mmol L^{-1}) (a) in the absence of 4-benzylpiperidine, (b) in the presence of 4-benzylpiperidine (5 mmol L^{-1}) at 25 °C for 1 min and (c) 60 min.

The decomposition of BA-BPD undergoes amine-catalyzed E1cB elimination reaction, which is amine-dependent. As shown in Figure s8, it is confirmed that the amine-catalyzed decomposition of BA-BPD successfully proceeds to generate 4-benzylpiperidine in the presence of DBU in solution as previously described, but autocatalytic process is not clear. The superbase DBU, as the photolysis product of QA-DBU, exhibits stronger reducibility, lower volatility as well as much more higher efficiency of amine-catalyzed decomposition than 4-benzylpiperidine. The above results indicate that BA-BPD can efficiently liberate the corresponding amine at 25 °C *via* not only autocatalytical decomposition but also superbase-catalyzed decomposition.

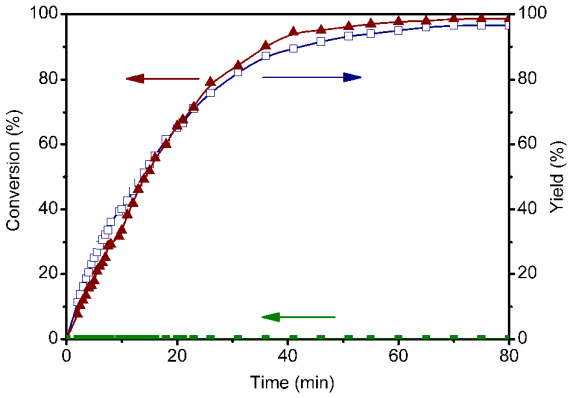

Figure s8 The conversion of BA-BPD (100 mmol L^{-1}) (▲) and the formation of dibenzofulvene (□) as a function of time in the presence of DBU (5 mmol L^{-1}), as well as the conversion of BA-BPD in the absence of DBU (■) in DMSO- d_6 at 25 °C.

4 Detection of 4-benzylpiperidine from amine amplifier (BA-BPD) in the polymer

ESI-MS was employed to detect the proliferative 4-benzylpiperidine from amine amplifier (BA-BPD) in the obtained polymer. As shown in **Figure s9**, the detection of protonated 4-benzylpiperidine$^+$ (m/z =176.1) after amine-catalyzed decomposition is the direct evidence for the formation of 4-benzylpiperidine from amine amplifier. The signal intensity of DBU$^+$ (m/z =153.3) is apparently smaller than 4-benzylpiperidine$^+$, which further confirm the autocatalytic decomposition of amine amplifier by the corresponding 4-benzylpiperidine.

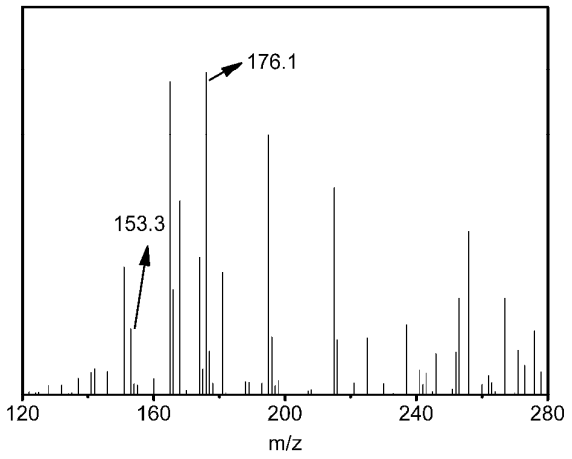

Figure s9 Positive ion ESI-MS spectra of polymer in DMSO solution. Experimental conditions: [QA-DBU] = 1.1×10^{-4} mol, [BA-BPD] = 1.65×10^{-4} mol, [BPO] = 5.5×10^{-4} mol, DMSO = 2.5 mL, TMPTA = 4 g, AA=1 g.

5 Reaction mechanism of BPO with 4-benzylpiperidine (BPD)

It has been well-established that redox initiation is highly effective in initiating free radical polymerization reactions, and the chemical mechanism has been adequately investigated. As shown in the **Scheme s2**, the chemical mechanisms for the interaction 4-benzylpiperidine/BPO can be presented according to the literature ((a) Denney D B, Denney D Z. *J. Am. Chem. Soc*, **1960**, *82,* 1389-1393. (b) Sarac A S. *Prog. Polym. Sci*. **1999**, *24*, 1149-1204.).

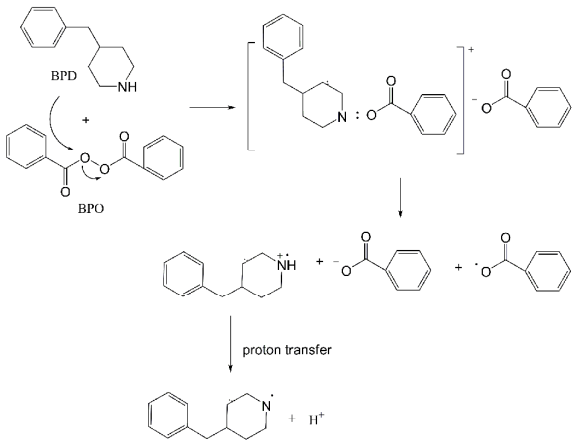

Scheme s2 Reaction mechanism of BPO with 4-benzylpiperidine (BPD)

6 ESR Spin Trapping (ESR-ST) Experiments.

For a better characterization of the efficiency on 4-benzylpiperidine/BPO, the spin-trapping technique has been used according to a procedure described in detail in ref (Tehfe M A, Dumur F, Graff B, et al. *Macromolecules* **2013**, *46*, 3761-3770). The ESR-ST experiments were carried out using an X-Band spectrometer (Bruker BioSpin, A300-10-12). To BPO in DMSO was slowly added 4-benzylpiperidine in DMSO, the radicals were produced, and then trapped by phenyl-*N*-*tert*-butylnitrone (PBN, TCI Company).

As shown in Figure s10, upon blending of 4-benzylpiperidine with BPO, the formation of the radicals is clearly observed in ESR spin trapping experiments.

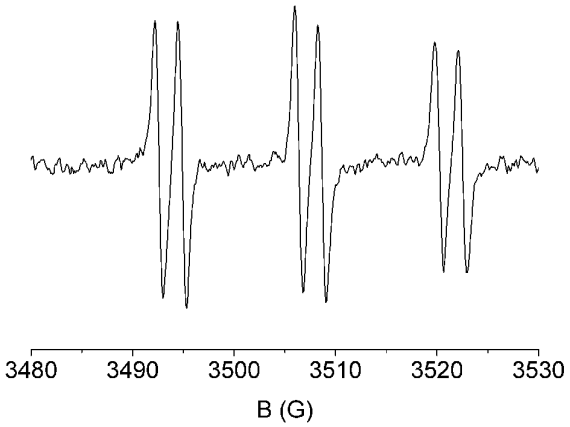

Figure S10 ESR-spin trapping spectrum of 4-benzylpiperidine/BPO in DMSO, [4-benzylpiperidine] = [BPO] = 0.003 M, [PBN] = 0.006 M.

7 FT-IR spectra of polymer based on chemical diffusion of amines for [BA-BPD]:[BPO] = 0.3:1 and calculation method of conversion

Double bond conversion was calculated by internal standard method. The area of the carbon-carbon double bonds at 810 cm^{-1} (A_{810}) was integrated and normalized by an internal standard peak at 1724 cm^{-1} (A_{1724}). The A_{810}:A_{1724} ratio was used to characterize the concentration of double bonds. The conversion was obtained using Equation 1.

$$Conversion = \left[1 - \left(\frac{A_{810}}{A_{1724}}\right)_t \Big/ \left(\frac{A_{810}}{A_{1724}}\right)_0\right] \times 100\% \qquad (1)$$

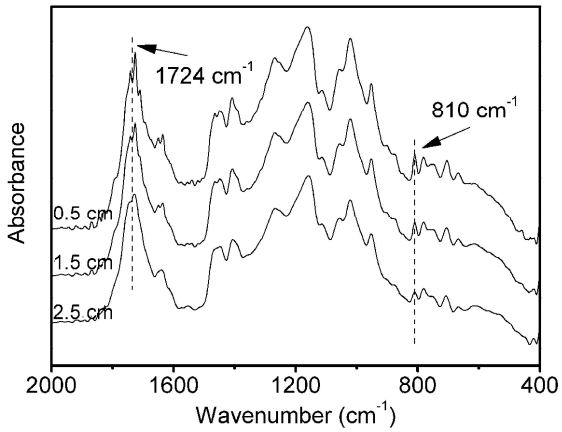

Figure s11 Spatial FT-IR spectra of polymer at different radii: (a) 0.5 cm, (b) 1.5 cm, (c) 2.5 cm.

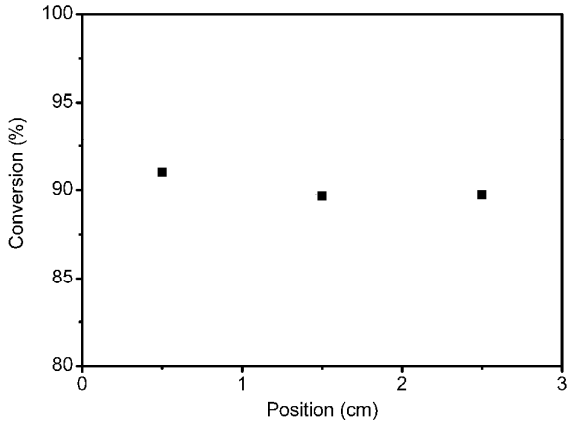

Figure s12 Conversion *vs* position at different radii: (a) 0.5 cm, (b) 1.5 cm, (c) 2.5 cm.

8 Hydroxyl functionalized carbon nanotubes (MWNT-OH)

Synthesis of MWNT-COOH

Into a 1000 mL flask equipped with a condenser, pristine MWNTs (12.0 g, 1.0 mol C), HNO_3 (65%, 100 mL, 1.465 mol), and H_2SO_4 (98%, 300 mL, 5.52 mol) were added with vigorous stirring. The flask was then immersed in an ultrasonic bath (40 kHz) for 10 min. The mixture was then stirred for 100 min under reflux (the oil bath temperature was increased gradually from 90 to 133 °C). A dense brown gas was evolved during this period, which was collected and treated with aqueous NaOH connected to the condenser by a plastic tube. After cooling to room temperature, the reaction mixture was diluted with 500 mL of deionized water and then vacuum-filtered through a filter paper (Fischer). The solid was dispersed in 500 mL of water and filtered again, and then 200 mL of water was used to wash the filter cake several times. The dispersion, filtering, and washing steps were repeated until the pH of the filtrate reached 7 (at least four cycles were required). The filtered solid was then washed with ca. 200 mL of acetone and THF five times to remove most of the water from the sample and dried under vacuum for 24 h at 60 °C, giving 7.2 g (↑ 60% yield) of MWNT-COOH.

Synthesis of MWNT-OH

The as-prepared MWNT-COOH (2.0 g) was reacted with excess neat $SOCl_2$ (50 mL, 0.685 mol) for 24 h under reflux (the temperature of oil bath was 65-70 °C). The residual $SOCl_2$ was removed by reduced-pressure distillation equipped with a liquid nitrogen trap, giving acyl chloride-functionalized MWNTs (MWNT-COCl). The as-produced MWNT-COCl was immediately re-acted without further purification with glycol (50 mL, 0.9 mol) for 48 h at 120 °C. Hydroxyl-functionalized MWNTs (MWNT-OH) (1.5 g) were obtained by repeated filtration and washing.

9 Photo-screened feature of functionally photo-screened materials containing carbon nanotube

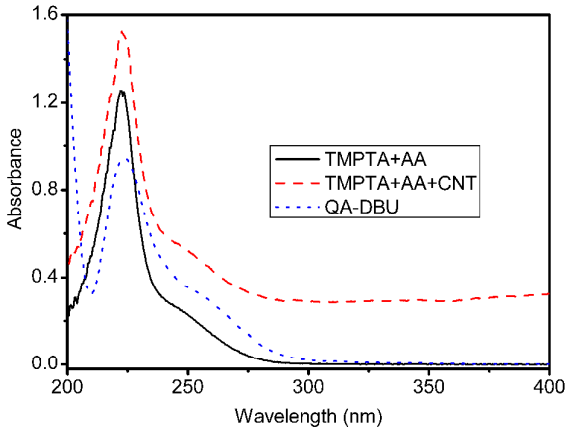

Figure s13 UV-Vis spectra of TMPTA & AA, TMPTA & AA & CNT, QA-DBU in AN.

Photo-screened feature of carbon nanotube in acetonitrile was investigated by UV-Vis Spectroscopy (Perkin Elmer Lambda 750). As shown in **Figure s13**, the absorption spectra of QA-DBU in acetonitrile (1×10^{-5} mol L^{-1}) shows a broad band at 200-300 nm with a dominant wavelength of 223 nm, and yet a strong absorption at 222 nm in the UV spectra of TMPTA &AA solution can also be observed, so just a broad absorption band at 228-300 nm with weaker absorption can be used for QA-DBU. But the addition of CNT leads to an obvious increase in absorption from 200 nm to 400 nm, resulting in the light not being able to penetrate into the solution, and thus the preparation of functionally photo-screened materials is one of the major challenges for photopolymerization.

10 Effect of peroxides on the self-propagating polymerization

Under the same conditions ([QA-DBU] = 1.1×10^{-4} mol, [BA-BPD] = 1.65×10^{-4} mol, [peroxide] = 5.5×10^{-4} mol, DMSO = 2.5 mL, TMPTA = 4 g, AA=1 g), peroxide reactivity impacts polymerization was investigated. Traditionally, the lower the stability of the peroxide, the faster the polymerization rate. Among the peroxides studied, IPP and BPO is the least stable initiator, suggesting more facile cleavage of O-O peroxide bonds, and hence rapidly triggered the self-propagating, whereas the other peroxides include DCP (dicumylperoxide), TBPB (tert-Butylperoxybenzoate) and CHP (cumenehydroperoxide) are so stable that the self-propagating polymerization cannot start.

Table s2. Half-life temperature peroxides[1]

Code	Chemical name	Half-life temperature (°C)		
		10 h	1 h	1 min
IPP	diisopropyl peroxydicarbonate	47	62	95
BPO	Dibenzoyl peroxide	72	92	133
TBPB	tert-Butyl peroxybenzoate	104	125	167
DCP	Dicumyl peroxide	116	136	175
CHP	cumenehydroperoxide	140	166	260

[1]The half-life is available from the literature (Gnanou Y, Fontanille M. *Organic and physical chemistry of polymers*. Wiley, 2008).